


Experiments on a single large particle segregating in bedload transport

Hugo Rousseau ^{1,*}, Julien Chauchat,² and Philippe Frey ¹

¹Université Grenoble Alpes, INRAE, UR ETNA, 38000 Grenoble, France

²Université Grenoble Alpes, LEGI, Centre National de la Recherche Scientifique, UMR, 5519 Grenoble, France



(Received 23 November 2021; accepted 17 May 2022; published 28 June 2022)

We performed experiments on a large particle segregating upward in turbulent bedload transport. The experiment was conducted in a narrow flume, fed with small glass beads and water. The large particle, called the intruder, was a glass bead plunged into the bed of smaller glass beads. Its ascent was tracked using image analysis methods. We performed 11 configurations using two Shields numbers and eight size ratios ranging from 1 to 5.3. For each configuration, the experiment was repeated from five to seven times in order to evaluate its repeatability. We found that the temporal ascent of the intruder exhibited two stages. At first, the intruder rose slowly with an intermittent motion. Then, a second stage was observed in which the intruder accelerated suddenly until it reached the top of the bed. While the kinematics of the second stage was found to be repeatable for a given configuration, it was not the case for the first stage. A transition in the size ratio was also observed. For size ratio close to unity, the ascent was much more intermittent than above a size ratio $r = 1.7$. Above the same value, the trajectory of the intruder (vertical displacement as a function of the streamwise displacement) became linear with a constant slope, independent of the Shields number and the size ratio. Based on observations, we proposed a segregation mechanism that could explain this linear trajectory.

DOI: [10.1103/PhysRevFluids.7.064305](https://doi.org/10.1103/PhysRevFluids.7.064305)

I. INTRODUCTION

In rivers and streams, the solid material carried by the water flow in contact with the river bed is called bedload transport. After one century of modern research [1] some phenomena involved in bedload transport are not entirely understood and limit our ability to improve significantly its modeling. Particularly, size diversity can lead to a surprising pattern with large particles lying on smaller ones, known as armoring [2]. This counterintuitive size reverse grading has been found to modify the sediment rate considerably [3,4] and is still poorly understood.

Bedload, consisting of saltating, rolling, or sliding particles, is a specific form of granular flow over an erodible bed. Saltating particles undergo rapid flights and mainly encounter each other through binary collisions like in a classical gaseous granular state. By contrast, particles rolling or sliding with enduring frictional contacts flow as a granular liquid. In this case, the shear strain rate is directly proportional to the applied shear stress and Maurin *et al.* [5] showed that the classical laws for dense dry granular flow are still valid. Finally, deeper in the bed, a quasistatic granular regime occurs. Displacements are very small and rearrangements are consequences of the nonlocal change in the network of chain forces [6]. From these observations, Frey and Church [7] concluded that size sorting, also called segregation, in bedload transport should be investigated in the framework of granular physics. The advances in this community could shed light on the segregation mechanisms.

*hugo.rousseau@geo.uzh.ch

In the physics of granular media, one of the first milestones in the understanding of grain-size segregation in gravity driven flows was reached with the work of Savage and Lun [8]. That study explained the segregation mechanism occurring in a size heterogeneous mixture of dry particles flowing under gravity as a “kinetic sieving” mechanism. The moving particles act as a random fluctuating sieve, in which small particles are more likely to percolate under the action of gravity than larger particles. This downward movement is balanced by an upward movement of the largest particles that was called “squeeze expulsion” and assumed to be not size preferential. According to Gray [9], kinetic sieving and squeeze expulsion are the dominant mechanisms for gravity driven segregation in dense sheared granular flows that are free to dilate. Both phenomena have been studied by van der Vaart *et al.* [10] using a shear cell experiment. An asymmetric behavior was observed between a small particle percolating among large particles and a large particle rising upward among small particles. The small particle moves discontinuously but percolates faster than the large particle which, in contrast, was found to segregate continuously. This difference suggests that squeeze expulsion could be a more subtle process than proposed by Savage and Lun [8]. Therefore, the mechanism responsible for the ascent of the large particle should be investigated.

In vibrated systems, this mechanism has been studied by Jullien *et al.* [11] and Duran *et al.* [12]. More recently, the segregation of a large intruder has been studied numerically in shear and gravity driven flows. Ding *et al.* [13], Guillard *et al.* [14], and van der Vaart *et al.* [15] studied the stress repartition around a large particle and observed that an asymmetric stress develops. An increase of stress compared to the hydrostatic pressure at the bottom front of the intruder was systematically evidenced. This idea is particularly interesting since the local increase of stress is linked to the idea of a squeeze mechanism. For Guillard *et al.* [16] and Jing *et al.* [17], in the presence of gravity, the pressure is the only source of asymmetry regardless of the configuration and should drive the segregation force. Based on this result, they proposed to model the segregation force as a lift force, i.e., proportional to the pressure gradient. Van der Vaart *et al.* [15] observed a velocity lag between the large segregating particle and its surrounding small particles and hence proposed a modified Saffman force responsible for the lift of the intruder. In contrast, Staron [18] did not observe a lift force and suggested that the rise of the intruder should result from force fluctuations having a stronger effect on the displacement when directed upward than downward. The different studies highlight that there is, for now, no consensus on the forces responsible for the ascent of a large particle.

Experiments on a segregating large intruder were performed by Trewhela *et al.* [19] with a large disk in a two-dimensional (2D) shear cell. To our knowledge, they were the first to discuss the notion of squeeze expulsion. Two segregation mechanisms were observed. For size ratios (large to small diameter noted r) below $r = 2$, the rotation of the large particle above a pivot small particle is responsible for the segregation. In contrast, for $r > 2$, the ascent is driven by the deformation of the granular matrix which allows small particles to percolate under the large particles, pushing it upward. The work of Trewhela *et al.* [19] suggests that, contrary to the assumption of Savage and Lun [8], the mechanism counterbalancing kinetic sieving is size dependent. This idea is supported by the work of Guillard *et al.* [16] and Jing *et al.* [17], who found that the segregation force was dependent on the size ratio, with a maximum force around $r = 2$.

To our knowledge, there are only a few experimental works on segregation in bedload transport. For a bidisperse granular bed, Frey and Church [7] and Dudill *et al.* [20] highlighted that kinetic sieving is the main size segregation mechanism for small particles to percolate in bedload transport and it could be responsible for armoring in rivers. Ferdowsi *et al.* [21] performed experiments on segregation of a collection of large particles in bedload transport under laminar flow for a size ratio $r = 2$. They investigated the dynamics of large particles and found that the ascent of the large particles occurs not only in the flowing layer but also in the quasistatic regime. Large particles segregating from the bottom to the granular surface developed an armored bed. They emphasized the necessity to investigate the segregation of large particles in less idealized configurations, particularly with a turbulent free surface flow. Therefore, in the present paper, the main objective is to provide a first dataset that evidences size segregation of a large particle in turbulent bedload transport. A

large range of parameters has been explored to highlight the key issues and confront our results against previous research that used different configurations. Because the experimental setup is very challenging, the focus is placed on the phenomenological behavior of the large intruder and a thorough investigation of statistical mechanisms is set aside.

In order to obtain a large dataset, we performed 58 experiments for two Shields numbers, i.e., dimensionless bed fluid shear stress, and several size ratios ranging from 1 to 5. Details on the experimental apparatus and the different configurations are presented in the first section. Then, in the second section, we present the temporal dynamics and the trajectory of the intruder. Interestingly, the latter is linear with a constant slope almost independent of the configuration. In the last section, these results are discussed in light of the previous studies and a simple mechanism to explain the linear trajectory at the granular scale is identified. Finally, the main results of the present contribution are summarized and perspectives on the modeling of segregation forces are presented.

II. EXPERIMENTAL SETUP AND METHOD

The experimental setup is sketched in Fig. 1. A 2-m-long flume is used with a fixed width $W = 15$ mm. An obstacle of 60-mm height is installed at the outlet of the flume to cause bed formation of a 60-mm-deep granular bed made of glass beads with diameter d_s . The slope is $\tan \zeta = 10 \pm 0.01\%$. The flume is fed with water using a constant head reservoir and the water flow rate Q_w is measured with an electromagnetic flow meter. Bead distributor K-Tron's Bulk Solids Pump loss in weight feeder provides a constant sediment rate. Spherical transparent glass beads of density 2500 kg/m^3 (type-M glass beads from Sigmund Lindner) are used to model sediments. This setup has been shown to reproduce sediment transport parameters in good agreement with classical semiempirical bedload formulas [22].

In order to investigate steep slope size segregation of a large intruder in bedload transport, a large opaque glass bead of diameter d_l of the same density, 2500 kg/m^3 , is introduced into the granular bed and tracked by image analysis. The experiment consists in recording the ascent of this intruder in the granular bed. Eight size ratios were used and for each we performed five to seven repetitions. It provides a satisfying balance between the number of parameters we wanted to investigate and the number of repetitions. For each experiment, we proceeded with the following steps.

(1) The sediment rate Q_s was fixed and the water flow rate Q_w was adjusted to find transport equilibrium with the bedline (top of the granular bed) parallel to the bottom of the flume. Then, the sediment rate and the water flow were stopped.

(2) The large intruder was manually deposited in order to have its center z_I at a depth between $1.5d_s$ and $4d_s$ below the top of the granular bed, which has a thickness noted h_b . Based on theoretical calculations, we made sure that for these initial depths the granular bed was not submitted to the Janssen effect. In order to deposit the intruder we stopped feeding the flume with water and grains and we dug a hole into the granular bed, using a rod. Ensuring the same initial depths for the intruders between the different repetitions was one of the greatest difficulties. Indeed, with our method it was difficult to be more precise than 1 or 2 mm on the initial position, i.e., up to the size of a diameter in the granular bed.

(3) The water and the granular supply were turned on again and 1 min was allowed to elapse so that initial rearrangements linked to bed preparation occurred and to reach the stationary state for the fluid and granular flow.

(4) Then, the experiment was recorded until the intruder reached the surface of the granular bed or went out of the field of view, also called the region of interest (ROI).

It is important to point out that performing experiments in a turbulent bedload configuration is very challenging for different reasons. First, this is because of the exponential particle velocity, shear rate, and inertial number (I) profiles [5]: as the segregation velocity was shown to depend on the dry inertial number I [23], the deeper the intruder, the longer the segregation duration and the longer the experiment will last. In order to limit each experiment to a maximum of 1 h, the intruder was never positioned deeper than $4d_s$ below the bed surface. At this depth, the intruder begins to

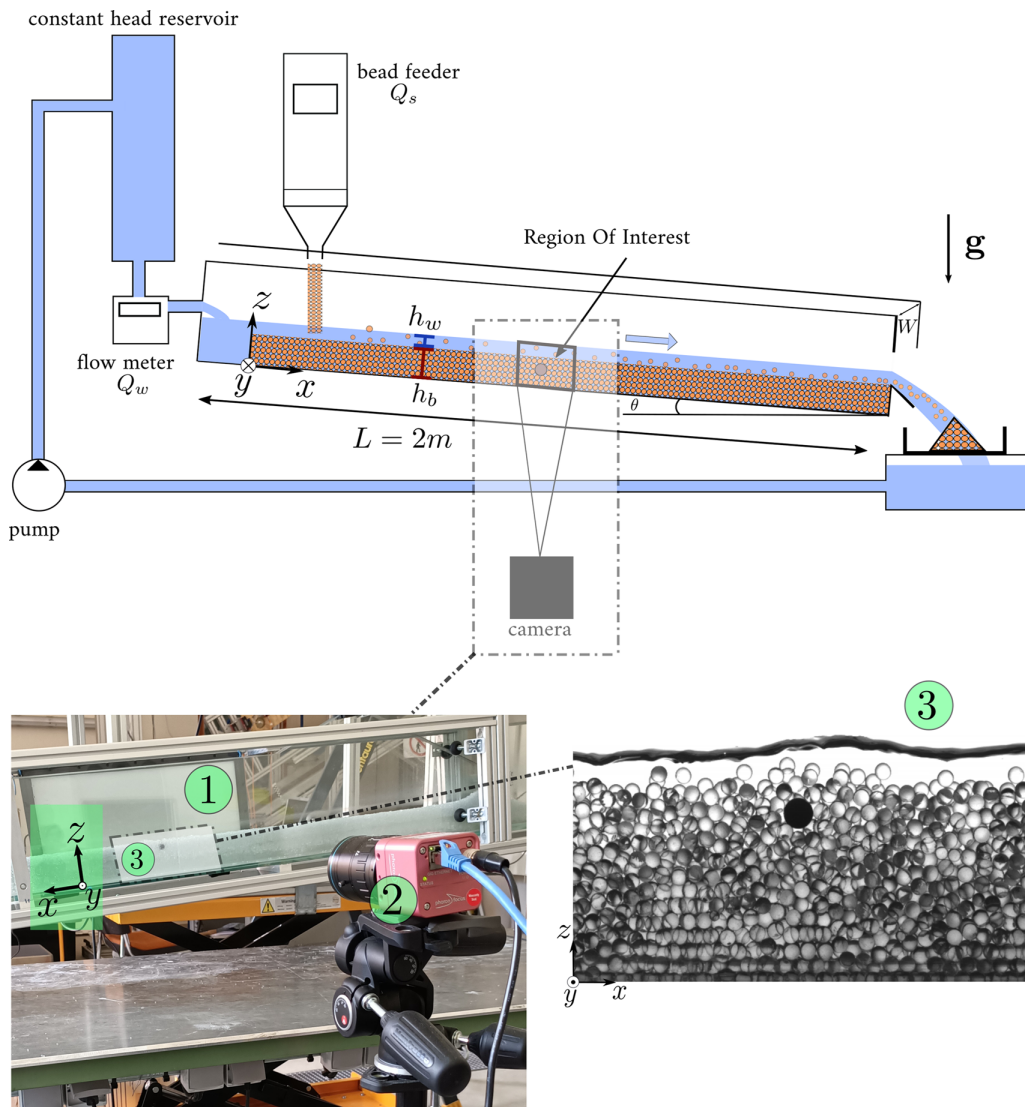


FIG. 1. Experimental setup at INRAE Grenoble laboratory. ① LED backlight. ② Camera used for recording. ③ Region of interest.

segregate in the quasistatic regime and finishes its ascent in the liquid flow regime. In the liquid regime, displacement of the intruder is supposed to be relatively fast, large, and regular. In contrast, in the quasistatic regime, displacements are small and irregular, due to long chain interactions. The displacement is expected to be more random, less identifiable, and thus more difficult to interpret.

Secondly, a transport equilibrium with the granular bed parallel to the water free surface had to be maintained. One could argue that the time and spatially averaged quantities should be the same from one repetition to another but the time and space variations of the turbulent flow and of the granular bed also impact the behavior of the intruder. Thus, even for a given configuration, all the repetitions were not submitted to exactly the same conditions. Lastly, the setup and the tools employed imposed constraints that determined the transport rate and the size ratios which could be

TABLE I. Summary of the configurations explored. The particle diameters are denoted by d_s and d_l , the fluid flow rate is denoted by Q_w , and the sediment transport rate is denoted by Q_s . The last column gives the number of repetitions for each configuration.

Configuration	d_s (mm)	W/d_s	d_l (mm)	r	Q_s (kg h ⁻¹)	Q_w (L s ⁻¹)	No. of repetitions
Sh1W1r1	5	3	5	1.0	16	0.075	5
Sh1W1r1.2	5	3	6	1.2	16	0.075	7
Sh1W1r1.7	5	3	8.6	1.7	16	0.075	6
Sh1W1r1.8	5	3	9.2	1.8	16	0.075	6
Sh1W1r2.5	5	3	12.7	2.5	16	0.075	7
Sh1W1r3.2	4	3.75	12.7	3.2	16	0.054	5
Sh2W2r2.5	2	7.5	5	2.5	30	0.065	6
Sh2W2r3	2	7.5	6	3.0	30	0.065	6
Sh2W2r4.3	2	7.5	8.6	4.3	30	0.065	5
Sh2W2r5.3	2	7.5	10.6	5.3	30	0.065	5

investigated. The transport rate is related to the dimensionless bottom fluid shear stress, also called the ‘‘Shields number’’:

$$\theta = \frac{R_{\text{BH}}S}{(s-1)d_s}, \quad (1)$$

where $S = \tan \zeta$ is the slope, $s = \rho^p/\rho^f$, and R_{BH} is a bottom hydraulic radius that takes into account the fluid dissipation on the sidewalls of the flume (see the Vanoni-Brooks method and Frey *et al.* [24]). Due to those dissipations and the fixed width of the flume, the best solution to vary the transport rate was to change the size d_s of the beads constituting the granular bed. A low Shields number $\theta = 0.13$ was investigated with $d_s = 5$ and 4 mm giving an aspect ratio between the flume width and the particle size: $W/d_s \approx 3$. Then, a higher value $\theta = 0.25$ was investigated by using $d_s = 2$ mm, corresponding to an aspect ratio $W/d_s = 7.5$.

The range of size ratios that could be investigated was determined by the aspect ratio W/d_s . Indeed, as it increases and as the size ratio gets close to 1, it is harder to track the intruder because it is hidden by surrounding particles of the bed. In this case, the intruder has to be placed against the wall to remain visible. However, for $W/d_s = 7.5$ this was not sufficient for the low size ratios since the intruder could move in the transverse direction (y direction). Considering these constraints, the different configurations that were performed and the number of repetitions are summarized in Table I. A configuration is defined by Sh (1 for the lowest Shields number or 2 for the highest), W (1 for $W/d_s \approx 3$ and 2 for $W/d_s = 7.5$), and the size ratio r . For all repetitions, the bulk Reynolds number $\text{Re} = 4U_w R_h/\nu$, where U_w is the mean velocity and ν the kinematic viscosity, is always above 4000, ensuring turbulent bedload transport. The Froude number $\text{Fr} = U_w/\sqrt{gh_w}$ is always higher than unity, meaning that the regime is supercritical. Finally, the Rouse number $\text{Ro} = w^s/\kappa u_\star$, where w^s is the vertical velocity of a small particle [25], $\kappa = 0.41$ is the von Kármán constant, and $u_\star = \sqrt{gR_{\text{BH}}S}$ is the shear velocity, is always higher than 2.5, meaning that there is no turbulent suspension but only bedload transport.

The experiment was recorded at 130 frames per second for $d_s = 5$ or 4 mm and 260 frames per second for $d_s = 2$ mm, with a Photon Focus camera provided by Alliance Vision. The ROI has a size 1024×500 pixels with a pixel resolution of 4.76 pixels/mm. A LED backlight panel was placed behind the ROI in order to provide constant and uniform light.

The opacity of the intruder among transparent beads combined with the high frequency recording allowed us to follow the position of the large particle thanks to a particle tracking velocimetry algorithm developed by Lafaye de Micheaux *et al.* [26] and previously used to track a large number of identical black beads [20,27].

The water surface and the bedline were also estimated following Lafaye de Micheaux *et al.* [26] and averaged over 1000 frames. The average bedline and free surface line obtained are shown for a

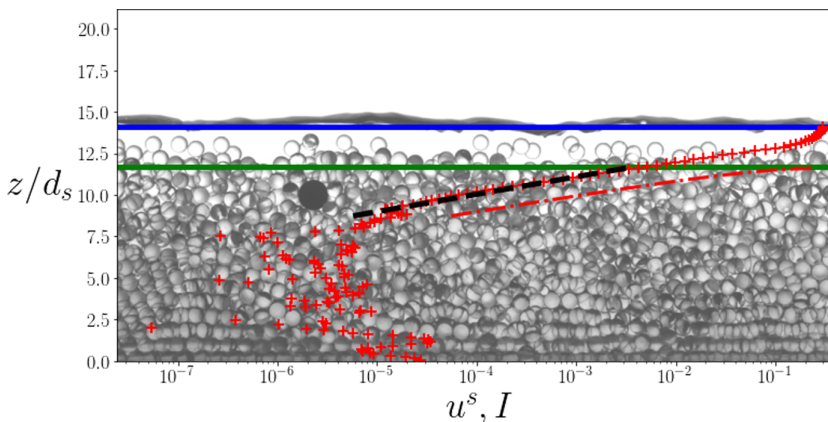


FIG. 2. Image of the ROI. The black particle is the large intruder of diameter d_I . The horizontal blue line (—) is the average free surface line and the green horizontal (—) line is the average bedline. Red crosses (++) correspond to the average streamwise velocity profile u^s , in m s^{-1} , of the granular bed measured with the *opyflow* toolbox. The black dashed line (---) is the linear fit. The red dash-dotted line (-.-) is the dry inertial number I .

typical experiment in Fig. 2 (see movieExperiment in the Supplemental Material for a video of this experiment [28]).

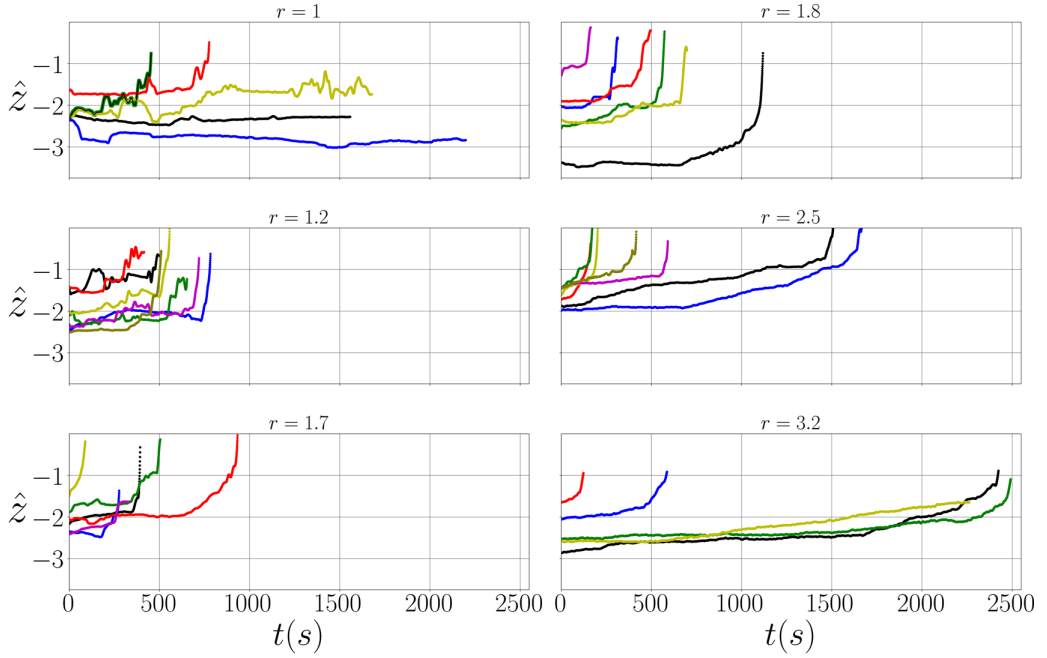
The particle streamwise velocity profile allows one to compute the granular shear rate $\dot{\gamma}(z)$. This profile is essential to link the segregation dynamics to the granular parameters. Particle tracking of the beads constituting the bed is not feasible since small particles overlap and are rarely identifiable. Moreover, a difficulty is that in the studied configuration, the particle streamwise velocity profile decays exponentially in the bed [5,29,30] spanning a large range of velocities and making it difficult to use classical particle image velocimetry techniques. To tackle this obstacle, the algorithm used by Rousseau and Ancy [31] was used. It is based on the resolution of the optical flow equation thanks to the Lukas-Kanade method. This algorithm was calibrated and validated in the context of our flume using the data of Frey *et al.* [30].

The obtained average particle velocity field (red cross) is shown in Fig. 2. The exponential velocity profile (linear in semilog plot) is recovered over more than four orders of magnitude. Deeper in the bed, the measurements are not possible since the grain displacements are not large enough over the experimental period. The dashed black line of Fig. 2 is the fit $u^s(z) = u_0 e^{z/d_0}$ on the particle streamwise velocity profile. Based on this fit, the granular shear rate is computed as $\dot{\gamma}(z) = du^s/dz$. Then, considering that below the bedline h_b the pressure is lithostatic, i.e., $P(z) = \Phi_{\max}(\rho^p - \rho^f)g(h_b - z)$ with $\Phi_{\max} \approx 0.58$, the dry inertial number $I = d_s \dot{\gamma}(z) / \sqrt{P(z) / \rho^p}$ [32] can be computed. According to Maurin *et al.* [5], the effect of interstitial fluid (water) on the granular rheology is negligible in bedload transport. They showed that the $\mu(I)$ dry granular rheology could also be used in bedload transport down to $I \approx 0.01$, suggesting that the rheology is local above this limit. The inertial number profile is plotted for the configuration shown in Fig. 2. The limit $I \approx 0.01$ is close to the bedline, indicating that the intruder effectively starts its ascent in the quasistatic regime and finishes in the granular liquid regime.

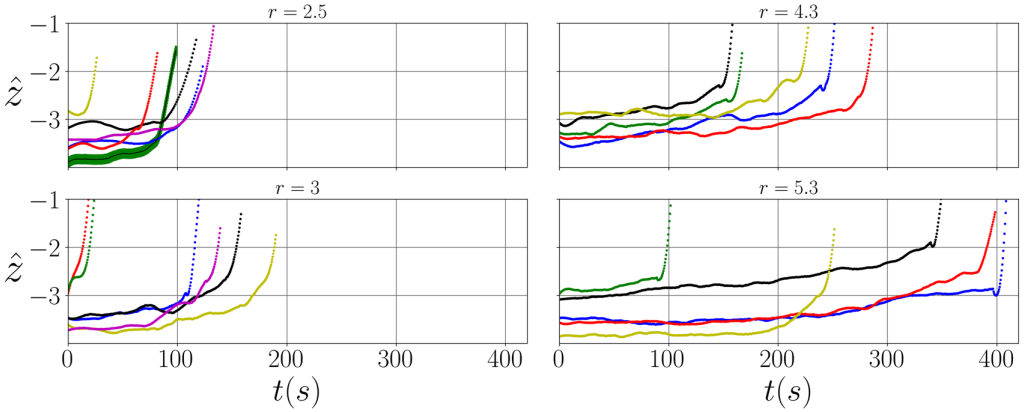
III. RESULTS

A. Vertical position with time

In Fig. 3(a) the depth of the center of the intruder $\hat{z}(t) = (z(t) - h_b)/d_s$ is plotted against time for configurations Sh1W1r1 to Sh1W1r3.2, corresponding to $\theta = 0.13$ (as an example, a repetition with



(a)



(b)

FIG. 3. Vertical position of the center of the intruder with time $\hat{z}(t) = (z(t) - h_b)/d_s$, for the different size ratios. (a) $\theta = 0.13$. (b) $\theta = 0.25$. The green envelope for configurations $r = 1$ with $\theta = 0.13$ and $r = 2.5$ with $\theta = 0.25$ corresponds to the potential error in the detection of the particle center. The thickness of this error bar is independent on the configuration [the difference between figures (a) and (b) is due to the difference of the diameter d_s in \hat{z}]. As a consequence, this envelope is not shown for each repetition. It avoids overloading the figures and makes each curve distinguishable.

configuration Sh1W1r1.8 is shown in the Supplemental Material [28]). For size ratios higher than $r = 1.2$, the intruders always segregate toward the top of the bed ($\hat{z} = 0$). The last position of each repetition corresponds to the last time step before the center of the intruder reaches the bedline. This instant will be considered as the final segregation time, denoted as t_{end} . This last vertical position

of the intruder is sometimes far from the bedline due to a display time step of 1 s between each position.

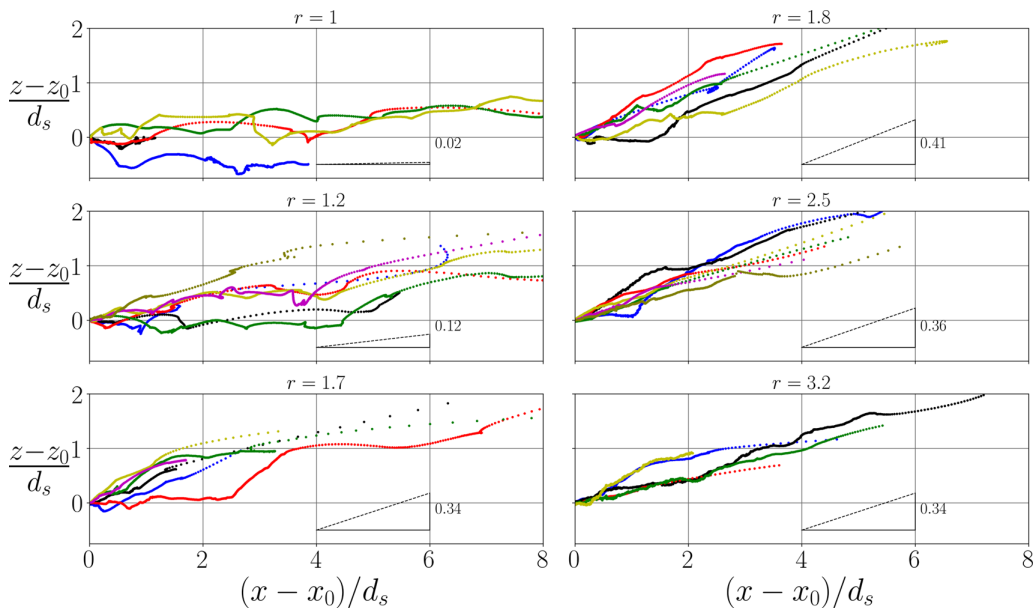
Two different stages are observed in the segregation dynamics of the intruder. At first, the intruder has a slow ascent characterized by a low vertical displacement. The intruder can remain at the same depth for a long duration before rising again, leading to an intermittent behavior. The deeper the initial depth, the longer the slow ascent. The deepest intruders can even stay at their initial vertical position for a very long time before beginning to rise slowly. Also, for repetitions having similar initial depths, the duration of the slow ascent regime varies from one repetition to another and the time for the intruder to segregate can differ, for example, by a factor of up to 5 for the case $r = 2.5$. Based on these raw data, it is difficult to conclude on the repeatability of the present experiments with the first stage being inherently stochastic.

In the second stage, the intruder kinematics drastically changes. It is characterized by a curvature corresponding to a sudden increase of the vertical acceleration. The curvature is defined as the convexity that breaks the slow ascent regime. After this point, the curve becomes linear and almost vertical, denoting a constant velocity before the intruder reaches the bed surface. Interestingly, for a given size ratio, the convexity does not always appear at the same depth. For example, in the case $r = 1.8$ (green curve) it appears two diameters below the bedline, while it appears three diameters below the bedline for the black curve. This suggests that the acceleration we observed is independent on the depth of the intruder. For a given size ratio, in most repetitions, the deeper the initial position, the longer it takes to reach the surface.

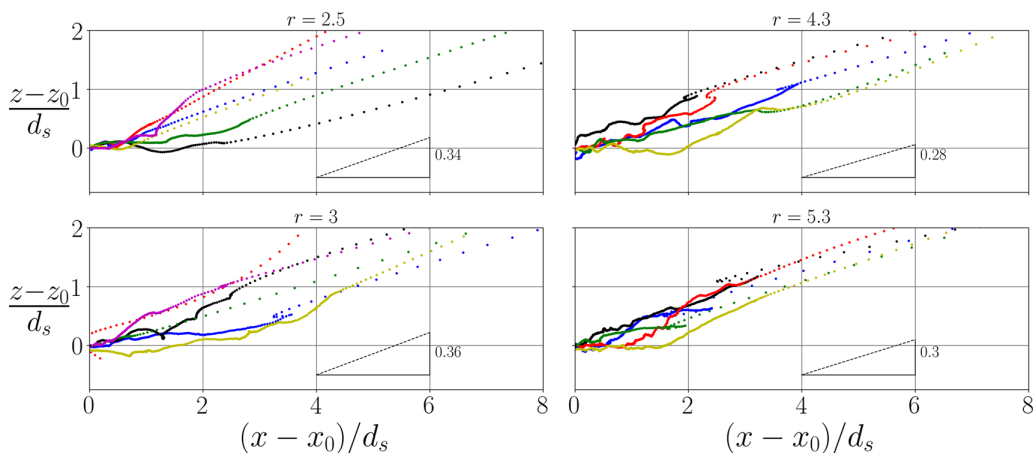
The same experiments have been carried out at a Shields number nearly twice higher ($\theta = 0.25$). For this value, experimental constraints allowed investigation only of size ratios higher than $r = 2$. The results are shown in Fig. 3(b) for configurations Sh2W2r2.5 to Sh2W2r5.3. The transition between the quasistatic and the granular liquid flow regime is located three diameters below the surface of the bed, while for a lower Shields number it was located only 1.5 diameters below. Doubling the Shields number has doubled the depth of the granular liquid flow regime, allowing us to study the behavior of the intruder deeper into the granular bed. For $r = 2.5$ and 3, there are, respectively, one and two repetitions for which the initial depth is located in the liquid regime [above the red area in Fig. 3(b)]. For these repetitions, the first stage of the ascent is not present. However, the second stage with a strong acceleration is still present. For the other repetitions, the two stages of the ascent are observed, showing that the shape of the $\hat{z}(t)$ curve was not due to the lowest Shields number we investigated.

Compared with the lowest Shields number, differences are observed in the segregation duration. First, for size ratios $r = 2.5$ and 3, the segregation durations are divided by almost one order of magnitude. As expected, when increasing the dimensionless bed shear stress, the intruder segregates faster. Secondly, for a given size ratio, one can see that the segregation duration can differ by a factor of 2 for repetitions with almost the same initial depth, suggesting that the variability is probably lower than in the configurations with a smaller Shields number. Nevertheless, note that this Shields number was obtained by doubling the value of the aspect ratio W/d_s . In granular flows, this parameter is known to affect the bulk streamwise velocity profile [33]. Therefore, the change we have observed in the segregation duration and the variability could also be affected by the modification of the aspect ratio.

While the phenomenology is the same for both Shields numbers with $r \geq 1.7$, this is not the case when looking at the small size ratios $r = 1$ and 1.2. For $r = 1.2$, the intruders rise toward the bed surface but the ascent is much more intermittent than for greater size ratios due to larger vertical fluctuations. For this reason, the curvature is less remarkable and thus the two stage dynamics is less evident. In configurations $r = 1$, the red and the green curve present the same phenomenology as for $r = 1.2$. In the other repetitions, the intruder position fluctuates around its initial position but it does not segregate within the observation time of the experiment. These observations indicate that a transition in the dynamics of the intruder exists between the low size ratios we have investigated and the size ratio starting from $r = 1.7$.



(a)



(b)

FIG. 4. Vertical displacement of the center of the intruder as a function of the streamwise displacement. The dashed line (----) corresponds to the averaged slope on all repetitions. (a) $\theta = 0.13$. (b) $\theta = 0.25$. x_0 and z_0 are for the initial position.

B. Spatial behavior

Investigation of the $\hat{z}(t)$ curve has revealed a high variability in the segregation duration that prevents us from concluding on the main parameters influencing the kinematics of the intruder. In addition, the difference of aspect ratio between both Shields numbers impaired assessing clearly the dependency on the Shields number. Hereafter, we propose to analyze the spatial behavior of the intruder. The results are less variable and exhibit an interesting behavior.

Figures 4(a) and 4(b) represent the vertical displacement $z(t) - z_0$ against the streamwise displacement $x(t) - x_0$ for both Shields numbers. For all size ratios higher than or equal to $r = 1.7$ it

is striking that the trajectories $z(x)$ exhibit a clear linear trend for both values of the Shields number. In some repetitions, the intruder can be advected in the streamwise direction without any vertical displacement. In such a case, the trajectory forms a horizontal plateau which is mainly observed at the beginning of the trajectories, before the intruder rises. In most of the repetitions with a size ratio above $r = 1.7$, this plateau is followed by a linear trajectory. This linearity shows that once the intruder has begun to move vertically, the streamwise movement of the particle is systematically associated with an upward vertical movement. In addition, the Shields number does not modify the linear behavior of the trajectory. For a given configuration, whatever the initial position of the intruder, linear trajectories tend to collapse, meaning that the linear ascent is somewhat universal. A fit on the trajectories allowed us to determine the mean slope. The order of magnitude is the same for both Shields numbers with a mean value around 0.3 and there is no obvious variation of this slope with the size ratio. This suggests that, whatever the initial depth, the size ratio or the Shields number, the slope of the linear trajectory is the same.

By contrast, for size ratios $r = 1$ and 1.2, in Fig. 4(a), the spatial behavior of the intruder is very different. The intruder moves spatially with successive ascents and falls resulting in a spatially random behavior with an intermittent ascent. For the case $r = 1.2$ the intruders have a tendency to rise higher than for the case $r = 1$, but the linear trajectory is broken by the descent of the intruder. In these configurations, the streamwise displacement is generally larger than for configurations with a linear trajectory. This indicates that the intruder has a greater propensity to be transported along the streamwise direction by advection and a lower probability to segregate vertically. This result is intuitively physically sound as the particles having $r \approx 1$ can be considered as tracers for the granular flow. As the size ratio increases, the streamwise advection is reduced and the spatial dynamics changes to the linear trajectory observed for larger size ratios. Our experimental results suggests that a change of phenomenology occurs in the range $r \in [1.2; 1.7]$.

IV. DISCUSSION

We propose a scaling for the $\hat{z}(t)$ curves which suggests that the intruder velocity is at first highly stochastic. Then, in the second stage the velocity appears much more reproducible. Beyond the variability, the dependency on the size ratio is also explored. Lastly, based on observations, we propose a mechanism which could explain the linear trajectory and we discuss it with the help of results from the literature in different configurations. Because of the challenging experimental setup described in Sec. II and our limited number of repetitions (5 to 7), the error bars are large so our interpretations must be taken with care. Therefore, in this section, the focus will not be placed on quantitative results but the aim is rather to highlight potential dependencies and propose new directions to better understand the segregation of a large intruder in bedload transport but also in more general configurations.

A. Segregation dynamics

In the results section, visual observations of the segregation of the intruder with time (see Fig. 3) suggest an exponential behavior for all experiments with size ratios starting from $r = 1.7$ and for some repetitions with a size ratio $r = 1.2$. In Fig. 5 these repetitions have been rescaled by the time t_{end} and the final position $z(t_{\text{end}})$. In order to focus on the convexity and the final part of the curves, where the ascent is rapid, only the last 60 s are shown. The semilogarithmic plot shows that, beyond the appearance, the vertical position does not rise exponentially with time. Nevertheless, the vertical velocity increases very rapidly as the intruder becomes closer to the surface, which is in line with the measured exponential streamwise particle velocity profile (see Fig. 2). In addition it suggests that the segregation velocity could indeed increase with the inertial number as found by Fry *et al.* [34] and Chassagne *et al.* [23].

For a given size ratio, curves show a similar behavior in the second stage of ascent. This suggests that the large variations of segregation duration are due to the first stage of segregation characterized

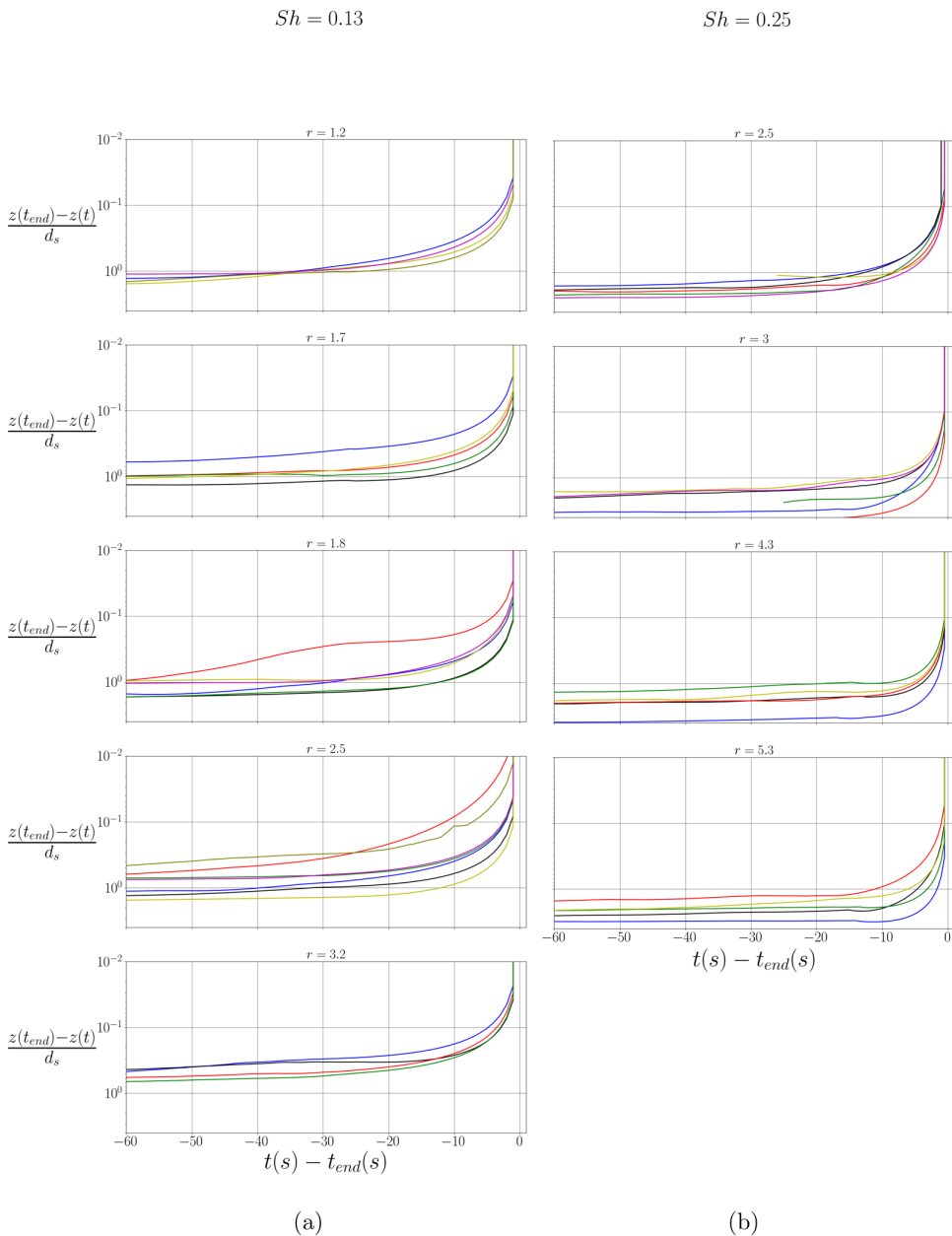


FIG. 5. Semilog plot of the intruder center elevation as a function of time, rescaled by the final time t_{end} , $z(t) - z(t_{\text{end}})$. The zero value on the horizontal axis represents the last time. (a) $\theta = 0.13$. (b) $\theta = 0.25$. Colors correspond to the same repetitions as in Fig. 3.

by a strong intermittent motion. The reason for the sudden vertical acceleration of the intruder is still an open question. We believe that the acceleration is not only due to state variables and that nonlocal effects are probably important as well. An additional effect linked to the initial arrangement around the intruder at the initial state may be possible as well. Our rescaling makes it possible to get rid of the stochasticity linked to this initial configuration.

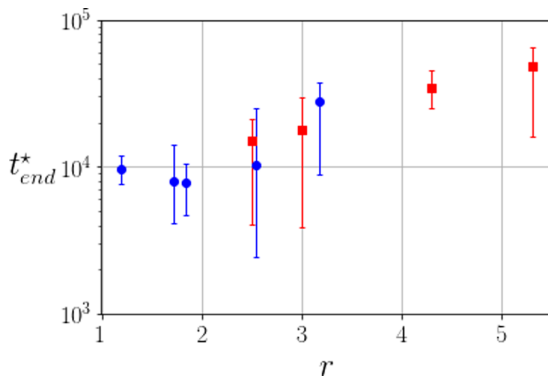


FIG. 6. Average segregation final dimensionless time t_{end}^* as a function of the size ratio r . Blue circles, $\theta = 0.13$; red squares, $\theta = 0.25$. Error bars give maximum and minimum segregation final times.

The two timescales we have observed were also observed by Ferdowsi *et al.* [21]. They linked the stochasticity appearing in the first stage to isotropic diffusion created by caging effects due to the network of forces appearing in the quasistatic regime. This isotropic diffusion could explain the first stage of the segregation dynamics.

Despite the high variability in the segregation duration, it is proposed to study the dependency on the size ratio for a given Shields number. For configurations explored in Fig. 5 (i.e., for intruders that segregate), the average final segregation time t_{end} can be nondimensionalized by the shear rate at the bedline $\dot{\gamma}_b(z = h_b)$ which is representative of the Shields number. This dimensionless final segregation time $t_{end}^* = t_{end}\dot{\gamma}_b$ is plotted as a function of the size ratio in Fig. 6. In order to analyze the segregation duration with the same initial depth, only an initial depth between $-1.5d_s$ and $-2.5d_s$ has been selected for $\theta = 0.13$ and between $-2.5d_s$ and $-3.5d_s$ for $\theta = 0.25$. The error bars give the extremum values obtained for each size ratio and can be very large for certain configurations but the dimensionless final segregation time t_{end}^* clearly shows that the segregation duration is dependent on the Shields number. Indeed, $\dot{\gamma}_b$ is higher for the case $\theta = 0.25$ than for the case $\theta = 0.13$ but the dimensionless final segregation times are of the same order of magnitude. Therefore, the higher the Shields number, the lower the segregation time.

In addition, for the size ratios in common with both Shields numbers, the collapse of the data suggests that the evolution of the dimensionless final segregation time with the size ratio does not depend on the Shields number, a point that would however warrant further studies.

For the lowest Shields number (blue circles), interestingly, a minimum or at least a threshold segregation duration seems to emerge around $r = 1.7$ and 1.8 . Such a result does not contradict Golick and Daniels [35], who observed, with shear cell experiments, a minimum segregation duration for $r \approx 2$, and Guillard *et al.* [16] and Jing *et al.* [17], who reported a maximum segregation force on a large intruder for $r \approx 2$. This suggests that the size ratio dependency of size segregation in bedload transport is similar to classical granular flow configurations.

B. Origin of the linear trajectory

The mean slope $\tan \alpha$, represented for each configuration in Figs. 4(a) and 4(b), is plotted as a function of the size ratio in Fig. 7. At $\theta = 0.13$, $r = 1.7$ and 1.8 correspond to size ratios for which a change of behavior is observed. Indeed, for $r = 1$ and 1.2 , the slopes are well below $\tan \alpha = 0.2$. In contrast, for higher size ratios, the slopes are almost always above this value and gather between 0.3 and 0.4 . In this section, we focus on those cases for which the linear trajectory with a constant slope always appears.

To the best of the authors' knowledge, the linear ascent trajectory was first reported by Duran *et al.* [12] in the case of a vibrated system. Vibrated configurations are usually considered to be

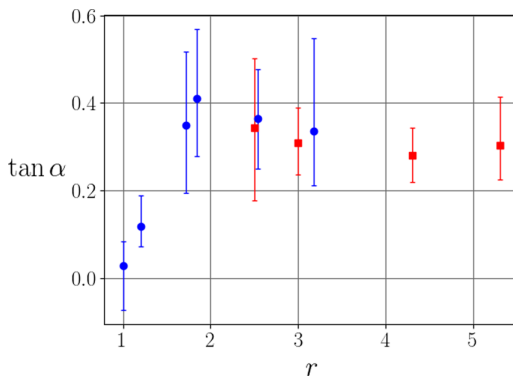


FIG. 7. Mean slope measured on the trajectories $z(x)$ for each size ratio. Blue circles, $\theta = 0.13$; red squares, $\theta = 0.25$. Error bars give maximum and minimum slope values.

different since the deformation of the medium is made by agitation which differs from sheared experiments as particles can encounter small flight. The trajectory being linear in both configurations, one could expect some possible similarities in the segregation mechanism. Duran *et al.* [12] made their experiment with a low deformation, that is to say, in the quasistatic regime. They argue that the observed linear trajectory was due to an arching effect where the intruder is carried by the arches created by the force chains in the quasistatic regime. Our linear trajectory could be observed either in the quasistatic or in the liquid granular flow regime, showing that it is not necessarily a consequence of the arches developing in the quasistatic regime.

Trajectories for all repetitions have been plotted in Fig. 8 and gather around the same slope. We performed a linear fit on the entire dataset of all repetitions. The black dotted line is the average slope obtained. It gives a value of $\tan \alpha = 0.34$ with a standard deviation measured as $\sigma(\tan \alpha) = 9.7 \times 10^{-2}$. The equivalent angle is $\alpha = 19.3^\circ$. Duran *et al.* [12] found the slope of the linear trajectory to be around 60° and mentioned that this angle corresponds to the 2D static angle of repose for monodisperse disks. In our flume, with $W/d_s = 7.5$, the critical angle of repose has been determined by measuring the angle at which the dry bed, made of glass beads, starts to flow continuously. This angle was found to be $\zeta_{\text{start}} = 26.6 \pm 1.2^\circ$ which is higher than the slope of $\alpha = 19.3^\circ$. This result

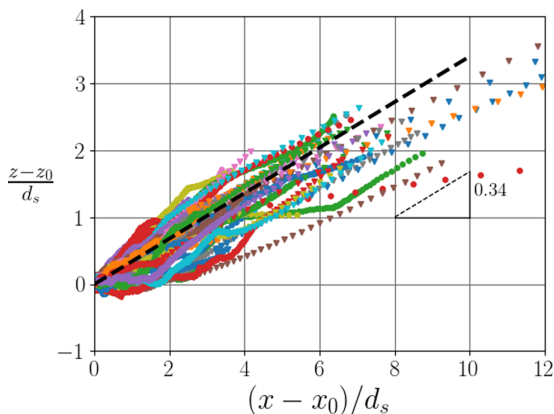


FIG. 8. Gathering of all the linear trajectories obtained experimentally. The black dotted line is the averaged slope measured. The standard deviation on the average slope is $\sigma(\tan \alpha) = 9.7 \times 10^{-2}$.

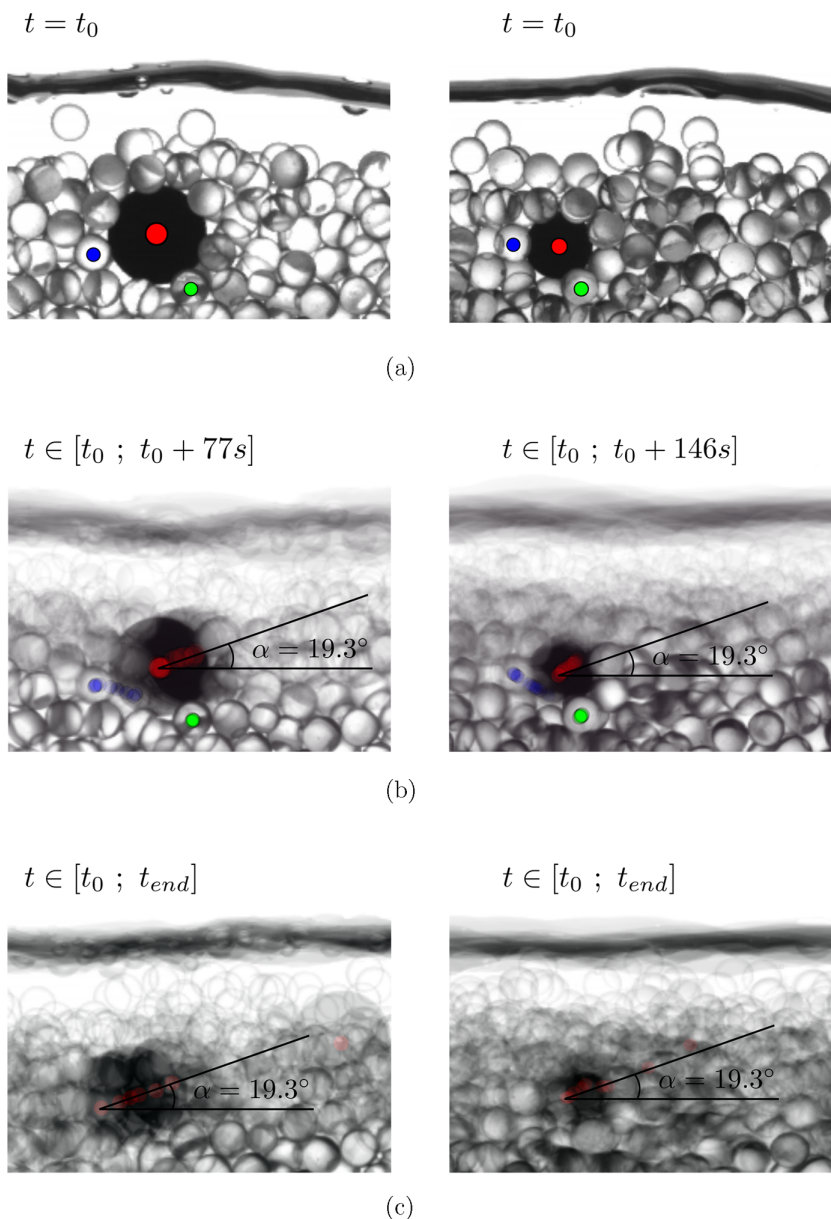


FIG. 9. (a) Initial layout before the observed mechanism occurs, for two repetitions with size ratio $r = 2.5$. (b) Mean image over a period $t \approx 70$ s, with one image every 7.7 s, after the initial layout presented in figure (a). The flow is from the left to the right. (c) Mean image over the whole experiment, for the two repetitions. The left column is for the size ratio $r = 1.8$ with $\theta = 0.13$ and corresponds to the repetition in green in Fig. 3(a). The right column is for the size ratio $r = 2.5$ with $\theta = 0.13$ and corresponds to the repetition in brown in Fig. 3(a).

suggests that, in our experiments, the slope of the linear trajectory is not controlled by the static angle of repose.

A typical segregation mechanism in Fig. 9 has been observed, which could be responsible for the linear trajectory. Two examples are given. The left column of Fig. 9 is for the size ratio $r = 1.8$

with $\theta = 0.13$ and corresponds to the repetition in green in Fig. 3(a). The right column of Fig. 9 is for the size ratio $r = 2.5$ with $\theta = 0.13$ and corresponds to the repetition in brown in Fig. 3(a). Figure 9(a) shows the initial layout before the process begins. The center of the intruder has been marked in red and two key particles have been marked in green and blue. Figure 9(b) represents the mean images over one period of the mechanism. It reveals the displacement of the intruder as well as the displacement of the two markers during the ascent of the intruder. In this image, the intruder segregates upward in the direction of the flow. The red points gather on a line having a slope similar to the averaged slope $\alpha = 19.3^\circ$. While the green marker at the bottom right does not move, the blue marker at the bottom left moves downward to the right. When the blue particle moves below the intruder it seems to push the intruder upward in the streamwise direction. The fact that the green marker does not move suggests that this contact could represent a pivot point over which the intruder is rolling, ultimately leading to an increase of the contact stress at the bottom right of the intruder. Such a local stress increase on the intruder was observed by Guillard *et al.* [14] and van der Vaart *et al.* [15] who reported an asymmetric stress originating from a complex circulation around the intruder and independent from the mean pressure. Ding *et al.* [13] also found a strong force asymmetry between the upper and the lower part of long intruders, with different cross sections, pulled into a granular bed. The maximum of the lift force was located at the bottom front of the intruder, for an angle of approximately 20° . This value is similar to the angle found for the trajectory of our intruder ($\alpha = 19.3^\circ$), suggesting that both values could be linked and that this angle could also correspond to the angle at which the green marker was observed to be a pivot point in Fig. 9(b). This suggestion has to be taken cautiously since the configuration of Ding *et al.* [13] is different. Pulling an intruder in a granular medium could induce a different circulation of the small particles around the intruder and the kinematics could be different. A thorough study of the contact forces around the intruder is necessary to support this comparison.

Finally, Fig. 9(c) shows the mean image over the whole experiment for both repetitions. The red points illustrate the linear trajectory observed and still gather on the 19.3° slope. We believe that the mechanism highlighted in Fig. 9(b) repeats, regardless of depth, until the intruder has completely segregated, giving the linear trajectory observed in Fig. 4. This suggests that the mechanism of segregation could be the same in the quasistatic regime and in the liquid regime.

When the size ratio increases, the number of neighbors around the intruder becomes larger and it is more difficult to observe the displacement of given surrounding particles. Nevertheless, since the angle of the linear trajectory seems to be independent of the size ratio (see Fig. 8), it suggests that the segregation mechanism in Fig. 9 could be universal. In Sec. III, it was observed that the only change with the size ratio was the time needed for the intruder to segregate. A possibility is that a large number of small particles need to move downward of the intruder to push it over the same height. Such an idea could be investigated in the future.

In this way, even if small particles can segregate downward more easily as the size ratio increases, the effect of each individual particle sneaking in below the intruder is less and less important on the intruder. Such an idea could argue in favor of the hypothesis of van der Vaart *et al.* [10] who reported an asymmetric velocity between small and large particles showing that the segregation behavior of a large particle was different from that of a small particle. This could also explain why Chassagne *et al.* [23] observed that the segregation velocity of the small particles increases exponentially with the size ratio while a maximum segregation efficiency at $r \approx 2$ is often observed for large particles that are segregating [16,17,35].

V. CONCLUSION

We have reported laboratory experiments of a single large particle segregating in bedload transport for various size ratios and two Shields numbers. All the intruders with size ratios higher than unity segregate. Nevertheless, starting from $r = 1.7$, the same temporal behavior is always observed. First, the intruder segregates slowly with intermittent motions. This dynamic is stochastic and seems to appear as soon as the initial position of the intruder is located in the quasistatic

regime. This stage was found to be responsible for the high variability in the segregation duration and could be highly dependent on the initial arrangement of small particles around the intruder. Then a sudden acceleration of the intruder appears and the latter segregates toward the top of the bed. This acceleration was found to happen at various depths and could be highly dependent on the arrangement around the intruder. Rescaling the position of the intruder by the final time of segregation showed that, for a given configuration, all the intruders have the same final kinematics regardless of the randomness linked to the first stage. The segregation duration was found to be minimum around a size ratio $r = 2$, confirming the results of Guillard *et al.* [16], Golick and Daniels [35], and Jing *et al.* [17] in our bedload configuration.

A surprising behavior was observed: the trajectory of the intruder was found to be linear with a constant slope regardless of the size ratio or the Shields number. Detailed experimental observations allowed us to understand the potential origin of the linear trajectory. When the intruder gets struck by a static fulcrum particle, a pushing small particle tends to lift the intruder and then moves beneath it, so the large particle moves forward and up. The repetition of this process could be responsible for the linear trajectory with constant slope. This mechanism is close to the one observed by Trehwela *et al.* [19] for disks in a shear cell for small size ratio ($r < 2$).

As a perspective, it would be necessary to improve statistical results. As an example, one could investigate the dependency on the segregation duration with the size ratio by focusing on one Shields number and performing more repetitions on each different size ratio. This should normally diminish the error bars and allow one to propose a quantitative dependency. Focusing on one configuration, it would be also possible to perform a large number of repetitions in order to analyze the stochastic behavior of the intruder in its first part of the ascent.

Another objective would be to analyze the physical origin of the linear trajectory of the intruder using a discrete element model and experiments in different flow configurations. A longer term objective would be to develop a Lagrangian model for the intruder on the model of Rousseau *et al.* [36]. The remaining open question is the expression of the forces exerted by the small particles on the intruder such as drag and lift forces.

All the data in this paper are available in Ref. [37].

ACKNOWLEDGMENTS

The authors are grateful to M. Church for reviewing and English corrections. H. Rousseau also acknowledges R. Maurin and R. Chassagne for fruitful discussions. This research was funded by the French Agence Nationale de la Recherche Project No. ANR-16-CE01-0005 SegSed, "Size segregation in sediment transport." The authors acknowledge the support of INRAE ETNA Labex Osug@2020 Investissements dAvenir Grant No. ANR-10-LABX-0056 and Labex TEC21 Investissements dAvenir Grant No. ANR-11-LABX-0030.

-
- [1] G. K. Gilbert and E. C. Murphy, *The transportation of debris by running waters*, U.S. Geological Survey Professional Paper No. 86, 1914 (unpublished).
 - [2] J. M. Buffington and D. R. Montgomery, Effects of sediment supply on surface textures of gravel-bed rivers, *Water Resour. Res.* **35**, 3523 (1999).
 - [3] R. I. Ferguson, K. L. Prestegard, and P. J. Ashworth, Influence of sand on hydraulics and gravel transport in a braided gravel bed river, *Water Resour. Res.* **25**, 635 (1989).
 - [4] D. R. Montgomery, M. S. Panfil, and S. K. Hayes, Channel-bed mobility response to extreme sediment loading at mount pinatubo, *Geology* **27**, 271 (1999).
 - [5] R. Maurin, J. Chauchat, and P. Frey, Dense granular flow rheology in turbulent bedload transport, *J. Fluid Mech.* **804**, 490 (2016).
 - [6] M. Houssais, C. Ortiz, D. Durian, and D. J. Jerolmack, Onset of sediment transport is a continuous transition driven by fluid shear and granular creep, *Nat. Commun.* **6**, 6527 (2015).

- [7] P. Frey and M. Church, Bedload: A granular phenomenon, *Earth Surf. Processes Landforms* **36**, 58 (2011).
- [8] S. B. Savage and C. K. K. Lun, Particle size segregation in inclined chute flow of dry cohesionless granular solids, *J. Fluid Mech.* **189**, 311 (1988).
- [9] J. M. N. T. Gray, Particle segregation in dense granular flows, *Annu. Rev. Fluid Mech.* **50**, 407 (2018).
- [10] K. van der Vaart, P. Gajjar, G. Epely-Chauvin, N. Andreini, J. M. N. T. Gray, and C. Ancey, Underlying Asymmetry within Particle Size Segregation, *Phys. Rev. Lett.* **114**, 238001 (2015).
- [11] R. Jullien, P. Meakin, and A. Pavlovitch, Three-Dimensional Model for Particle-Size Segregation by Shaking, *Phys. Rev. Lett.* **69**, 640 (1992).
- [12] J. Duran, J. Rajchenbach, and E. Clément, Arching Effect Model for Particle Size Segregation, *Phys. Rev. Lett.* **70**, 2431 (1993).
- [13] Y. Ding, N. Gravish, and D. I. Goldman, Drag Induced Lift in Granular Media, *Phys. Rev. Lett.* **106**, 028001 (2011).
- [14] F. Guillard, Y. Forterre, and O. Pouliquen, Lift forces in granular media, *Phys. Fluids* **26**, 043301 (2014).
- [15] K. van der Vaart, M. P. van Schrojenstein Lantman, T. Weinhart, S. Luding, C. Ancey, and A. R. Thornton, Segregation of large particles in dense granular flows suggests a granular Saffman effect, *Phys. Rev. Fluids* **3**, 074303 (2018).
- [16] F. Guillard, Y. Forterre, and O. Pouliquen, Scaling laws for segregation forces in dense sheared granular flows, *J. Fluid Mech.* **807**, R1 (2016).
- [17] L. Jing, J. M. Ottino, R. M. Lueptow, and P. B. Umbanhowar, Rising and sinking intruders in dense granular flows, *Phys. Rev. Research* **2**, 022069(R) (2020).
- [18] L. Staron, Rising dynamics and lift effect in dense segregating granular flows, *Phys. Fluids* **30**, 123303 (2018).
- [19] Tomás Trehwela, J. M. N. T. Gray, and Christophe Ancey, Large particle segregation in two-dimensional sheared granular flows, *Phys. Rev. Fluids* **6**, 054302 (2021).
- [20] A. Dudill, H. Lafaye de Micheaux, P. Frey, and M. Church, Introducing Finer Grains Into Bedload: The Transition to a New Equilibrium, *J. Geophys. Res.* **123**, 2602 (2018).
- [21] B. Ferdowsi, C. P. Ortiz, M. Houssais, and D. J. Jerolmack, River-bed armouring as a granular segregation phenomenon, *Nat. Commun.* **8**, 1363 (2017).
- [22] V. Hergault, P. Frey, F. Métivier, C. Barat, C. Ducottet, T. Böhm, and C. Ancey, Image processing for the study of bedload transport of two-size spherical particles in a supercritical flow, *Exp. Fluids* **49**, 1095 (2010).
- [23] R. Chassagne, R. Maurin, J. Chauchat, J. M. N. T. Gray, and P. Frey, Discrete and continuum modelling of grain size segregation during bedload transport, *J. Fluid Mech.* **895**, A30 (2020).
- [24] P. Frey, M. Dufresne, T. Bohm, M. Jodeau, and C. Ancey, Experimental study of bed-load on steep slopes, in *River Flow 2006, Lisbonne, PRT, 6-8 Septembre 2006* (Balkema, 2006), pp. 887–893.
- [25] R.I. Ferguson and M. Church, A simple universal equation for grain settling velocity, *J. Sediment. Res.* **74**, 933 (2004).
- [26] H. Lafaye de Micheaux, C. Ducottet, and P. Frey, Multi-model particle filter-based tracking with switching dynamical state to study bedload transport, *Machine Vision and Applications* **29**, 735 (2018).
- [27] A. Dudill, P. Frey, and M. Church, Infiltration of fine sediment into a coarse mobile bed: A phenomenological study, *Earth Surf. Processes Landforms* **42**, 1171 (2017).
- [28] See Supplemental Material at <http://link.aps.org/supplemental/10.1103/PhysRevFluids.7.064305> for a video and example of this experiment.
- [29] R. Chassagne, P. Frey, R. Maurin, and J. Chauchat, Mobility of bidisperse mixtures during bedload transport, *Phys. Rev. Fluids* **5**, 114307 (2020).
- [30] P. Frey, H. Lafaye de Micheaux, C. Bel, R. Maurin, K. Rorsman, T. Martin, and C. Ducottet, Experiments on grain size segregation in bedload transport on a steep slope, *Adv. Water Resour.* **136**, 103478 (2020).
- [31] G. Rousseau and C. Ancey, Scanning PIV of turbulent flows over and through rough porous beds using refractive index matching, *Exp. Fluids* **61**, 172 (2020).
- [32] F. da Cruz, S. Emam, M. Prochnow, J.-N. Roux, and F. Chevoir, Rheophysics of dense granular materials: Discrete simulation of plane shear flows, *Phys. Rev. E* **72**, 021309 (2005).

- [33] P. Jop, Y. Forterre, and O. Pouliquen, Crucial role of sidewalls in granular surface flows: Consequences for the rheology, *J. Fluid Mech.* **541**, 167 (2005).
- [34] A. M. Fry, P. B. Umbanhowar, J. M. Ottino, and R. M. Lueptow, Diffusion, mixing, and segregation in confined granular flows, *AIChE J.* **65**, 875 (2019).
- [35] L. A. Golick and K. E. Daniels, Mixing and segregation rates in sheared granular materials, *Phys. Rev. E* **80**, 042301 (2009).
- [36] H. Rousseau, R. Chassagne, J. Chauchat, R. Maurin, and P. Frey, Bridging the gap between particle-scale forces and continuum modelling of size segregation: Application to bedload transport, *J. Fluid Mech.* **916**, A26 (2021).
- [37] See <https://doi.org/10.5281/zenodo.6573845>.